

SVD enhanced seismic interferometry for traveltimes between microquakes

Gabriela Melo* & Alison Malcolm

Earth Resources Laboratory - Earth, Atmospheric, and Planetary Sciences Department - MIT

SUMMARY

In general, Green's functions obtained with seismic interferometry are only estimates of the true Green's function, introducing uncertainties to the information recovered from them. However, there are still many cases in which the source-receiver geometries are suitable for seismic interferometry, usually allowing the recovery of kinematic information. Here we show how to use the singular value decomposition to reinforce the accuracy of traveltimes obtained from interferometric Green's functions. We apply the combination of seismic interferometry and the singular value decomposition to obtain physically accurate inter-event traveltimes for microquake pairs at a geothermal reservoir. With a synthetic example, we show that the P-wave phase and coda-wave energy information are closer to correct with the singular value decomposition than without. These traveltimes could be used for velocity tomography and event location algorithms to obtain more accurate event locations and locally accurate velocity models.

INTRODUCTION

To recover the full Green's function (GF) between two receivers using seismic interferometry (SI) requires that these two receivers be surrounded by a surface of both monopole and dipole sources. Even if one is interested in obtaining only accurate estimates of traveltimes, this still requires full (monopole) source coverage, a condition which is rarely met in practice. As a result, we generally recover only estimates of the true GF, which introduces uncertainties to the information recovered from these empirical (interferometric) Green's functions, that here we refer to as EGFs. Even though most practical scenarios are not ideal, there are many cases in which the source-receiver geometry is suitable for SI, allowing for the recovery of at least some information (generally kinematic) from the EGF. Snieder (2004) showed that the sources that give the main contribution to the EGFs are the ones located along the ray path between the two receivers, and those in the Fresnel zone around these sources. This conclusion comes from the method of stationary phase; the sources along the raypath are the sources for which the phase of the receiver crosscorrelations is stationary. From this argument, assuming full source coverage, energy emanated by sources outside the Fresnel zone should cancel. Thus, as long as we have sources and receivers on stationary paths, we have a good chance of being able to apply SI to recover traveltimes information.

In order to improve the accuracy of EGFs for cases with gaps in the source coverage, Melo et al. (2010) introduce a method in which they use the singular value decomposition (SVD) (see e.g. Golub and van Loan (1996)) to enhance EGFs. SVD is a numerical technique commonly used in seismic data pro-

cessing (see e.g. Ulrych et al. (1988); Sacchi et al. (1998)), to increase the signal to noise ratio and filter linear events. Melo et al. (2010) show that EGFs obtained by stacking lower-rank approximations of crosscorrelograms, obtained through SVD, have enhanced physical arrivals that are not properly recovered using the standard stacking in SI. The idea behind this technique is that the stationary and non-stationary energy in the crosscorrelograms generally have different signatures that, under favorable circumstances, can be separated through SVD. Stationary energy in the crosscorrelogram is characterized by linearity, coherency, low wavenumber, and thus nearly in-phase energy along the source dimension. Non-stationary energy by contrast is characterized by non-linearity, incoherency, high wavenumber, and out-of-phase events along the source dimension. The relationship between frequency (or source-wavenumber in our case) and singular values is key to understanding why SVD is able to separate stationary and non-stationary energy. Hansen et al. (2006) explain this relationship - large singular values correspond to low frequencies and small singular values correspond to high frequencies. As they correspond to low-frequencies, large singular values are associated with events that are in phase in the crosscorrelogram, coming from stationary sources whose energy contribute to the EGF. In the context of waveguides, for instance, Philippe et al. (2008) exploit this connection between singular values and frequency for characterization of targets. They show that the first singular value associated with a given target is proportional to the backscattering form function of the target, and that the second singular value is proportional to the second derivative of the angular form function. They then use SVD to extract the backscattered frequency signature of a target in a waveguide.

Here the goal is to use the SI-SVD method to obtain accurate traveltimes estimates between a pair of microquakes. Curtis et al. (2009) show that, by reciprocity, while most applications of SI estimate the GF between two receivers surrounded by sources, it is also possible to use SI to estimate the GF between a pair of sources. The sources in our particular case will be microquakes recorded at a geothermal reservoir. Some of the challenges in working with microseismic data are gaps in the receiver coverage, uncertainties in the source locations, and low signal-to-noise ratio. These challenges will generally result in errors in the EGF. To alleviate some of these problems, Melo and Malcolm (2011) use the SVD technique for estimating the EGFs. Their acoustic modeling results indicate that, in some cases where microseismic data is highly contaminated by noise, SVD gives an accurate estimate of the EGF even when the standard technique fails to converge. They also suggest that, in general, the phase of direct wave and the coda energy are closer to correct with SVD than without. Finally, they demonstrate that as well as stability with respect to noise, this method is also stable with respect to the aperture of the source coverage, which is important because errors in the location of microquakes can be significant.

SVD enhanced interferometric traveltimes

G appears strongly contaminated by noise and neither the direct arrival nor the coda wave are visible. Also, fluctuations and random noise are strongly attenuated in G_1 , revealing not only the direct arrival but also reducing the noise to be close to the coda wave level. The phase differences between G and G_1 and G_{ref} are 0.2850 and 0.0015 s, respectively. The relative errors in the L_2 -norm of the coda are 148% for G and 11% for G_1 . We see that SVD eliminates most of the noise in the coda wave, as well as the fluctuations before the direct wave, illustrating its stability with respect to noise.

GEOHERMAL FIELD DATA

We now apply the SI-SVD method to a real microseismic dataset from a geothermal field. Figure 3 shows 2D projections of the distribution of a set of microquakes, red dots, and the receivers, blue triangles. The microquake locations are preliminary estimates obtained with a rough 1D approximation of the real velocity model. The source-receiver geometry is similar to the synthetic example presented above. We estimate P-wave traveltimes between pairs of microquakes, with the goal of ultimately using these traveltimes as inputs for velocity tomography and microquake location code, to obtain a high-resolution velocity model and accurate event locations in the microquakes nest area.

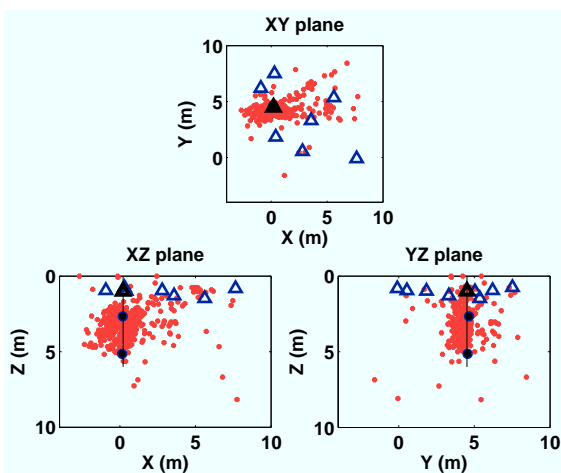


Figure 3: Two-dimensional projections of microquake (red dots) and receiver (blue triangle) locations in the standard XY -, XZ -, and YZ -planes. The receiver and the pair of events in black are in a near-stationary configuration.

In figure 3, we see a nest of microquakes that seems to come from directly below one of the receivers (marked in black), which, we refer to as the stationary receiver R_s (note that R_s , in general, is not exactly but near a stationary location with respect to a microquake pair). We now choose pairs of microquakes (e.g., the two microquakes marked in black in figure 3) that are nearly on a stationary path with R_s . For simplicity, we choose the direction of the stationary path to be parallel to the Z -axis (black line coming off of R_s in figure 3). We choose

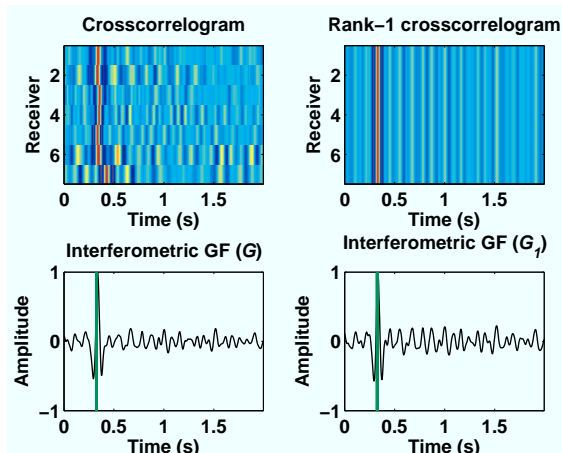


Figure 4: The original (left) and rank-1 (right) crosscorrelograms are on the top. On the bottom, the black curves are the EGFs, G and G_j , and the red curve is reference GF, G_{ref} , and the vertical green line indicates the traveltime based on the P-wave arrival. G and G_1 agree well, indicating that there is enough stationary energy in the crosscorrelograms, suggesting that the kinematic information is reliable.

many pairs near this stationary path and for each pair we estimate the P-wave traveltimes in four different ways: i) since the microquakes and R_s are nearly along a stationary path, we subtract the P-wave arrival times picked in the recorded data; ii) standard SI (crosscorrelation and stack of the vertical-component signal for all receivers); iii) SI-SVD method (stack of lower-rank crosscorrelogram over the receivers); iv) cross-correlation of vertical component for R_s only. For measurements ii), iii), and iv), the traveltime will be the peak of the (stacked) crosscorrelations. If the microquakes and R_s are along an exactly stationary path, then all four estimates should be equal. Figure 4 shows original and rank-1 crosscorrelograms and the respective crosscorrelogram stacks for a microquake pair. In this case, the signal-to-noise ratio is good and both G and G_1 are similar, suggesting that the kinematic information is reliable. This is often the case for the waveforms of the events in figure 3, but it is not the case for the entire dataset. Note that the crosscorrelation stacks (EGFs) here do not actually converge to the true GF.

Since the pair of microquakes and R_s are nearly along a stationary path, the true P-wave traveltime between any two events should approach the difference between the traveltimes of the P-waves recorded at R_s , which is our measurement i). Thus, we use these traveltimes as the reference traveltimes. Now, we investigate the correlation between the three traveltime estimates - ii), iii), and iv) - and the reference one - i). Figure 5 shows cross-plots for these traveltimes. Even though all three cases show some deviated points (the ones farther away from the trend line), the estimates obtained via SI and SI-SVD correlate better with the P-wave traveltimes than the estimates obtained using signal from R_s only. This suggests that inter-event traveltime estimates for this dataset based solely on crosscorrelation at one station may have large errors. Thus, in

SVD enhanced interferometric traveltimes

this case, the stacking step in estimates ii) and iii) is important for the convergence of the traveltimes.

We can think of a few ways to classify a given traveltime estimate as accurate enough or not. One could remove the deviated points of one and/or another of the different estimates (blue, red, and black in figure 5) or, alternatively, of all of them for a more conservative approach. Since here we are also investigating the use of SVD in SI, we remove the scattering only from red estimates in figure 5. Removing the seven red deviated points in figure 5 we obtain figure 6. As mentioned above, the signal-to-noise ratio in this data set is generally good, leading to relatively sharp crosscorrelations in general. However, the three deviated data points in figure 6 are exceptions. Figure 7 shows the SI results for one of the blue deviated points in figure 6. Similar to the synthetic example, in this case the crosscorrelograms are fairly different (as are the respective EGFs) indicating a high level of incoherency in the crosscorrelograms. However, G_1 still peaks at a reasonable time shift, as seen in figure 6, which indicates that the result based on SVD for this case is reasonable. It is important to note that we do not expect estimates ii), iii), and iv) to coincide perfectly with the traveltimes based on the P-wave picks (but we expect it to be close) for a few reasons. First,

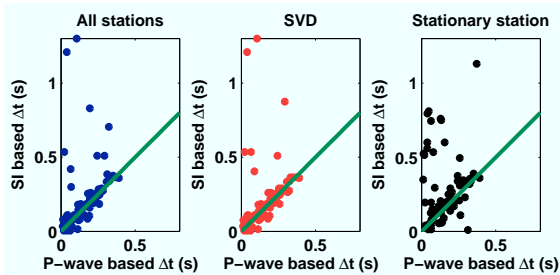


Figure 5: Cross-plots showing the correlation between the estimated and reference traveltimes for P-waves. The green line is the slope-1 line that crosses the origin. The first two estimates, obtained through SI, have less scattering than using signal from R_s only.

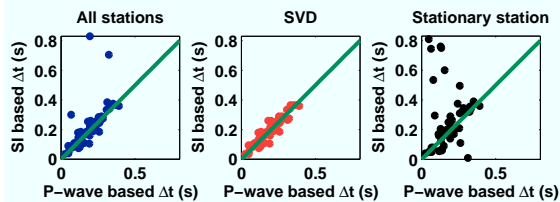


Figure 6: Similar to figure 5 but the red deviated points in the SVD estimates were removed.

the sources and receivers are not located on exactly stationary paths. As said above, the microquake locations here were obtained with a rough velocity model so there are likely errors in the event locations, which lead to uncertainties in whether the sources are actually located near stationary paths. However, the SI-SVD method is stable with respect to these location er-

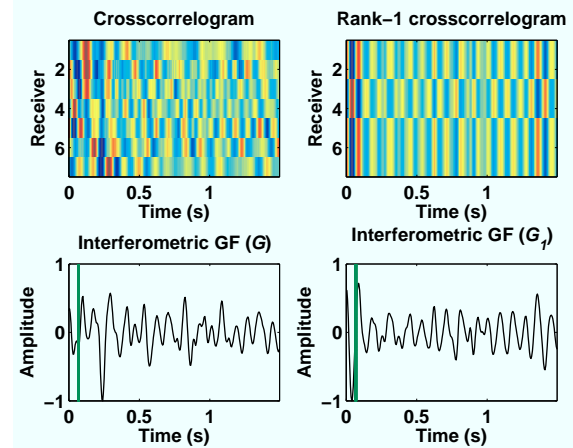


Figure 7: The original (left) and rank-1 (right) crosscorrelograms are on the top. On the bottom, the black curves are the EGFs, G and G_j , and the red curve is reference GF, G_{ref} , and the vertical green line indicates the traveltime based on the P-wave arrival. G and G_1 are different, indicating a high level of incoherency in the crosscorrelograms. However, G_1 peaks at a reasonable time shift as measured by its relationship to the difference time pick figure 6.

rors as long as the events are within the Fresnel zone. Second, low signal-to-noise ratios are also a source of errors. We did not exclude data with low signal-to-noise ratio from our analysis because we expected SI-SVD to be able to give the correct peak on the EGF in some of these cases, as is indeed the case as mentioned above. Given these uncertainties, we the correlation between SI-SVD and P-wave based traveltimes is generally good, making the method promising for improving estimated locations and velocities.

Conclusions and future work

We have shown that physically accurate inter-events traveltime estimates are obtained, for microquake pairs of a geothermal reservoir, through a combination of SVD and SI. We have illustrated this both with synthetic and field data examples. These traveltimes can be used in velocity tomography and microquake location algorithms, to obtain locally high-resolution velocity models and accurate event locations in the area of the microquake nest. While the SI-SVD technique in general may lead to more accurate estimates of inter-events traveltimes, it can only be applied to sets of sources and receivers in near-stationary paths.

Acknowledgments

We would like to thank Oleg Poliannikov and Michael Fehler for great suggestions during our discussions. This work is supported by grants from the Department of Energy (DE-FG36-08GO18197) and the founding members consortium at Earth Resources Laboratory (ERL).

EDITED REFERENCES

Note: This reference list is a copy-edited version of the reference list submitted by the author. Reference lists for the 2011 SEG Technical Program Expanded Abstracts have been copy edited so that references provided with the online metadata for each paper will achieve a high degree of linking to cited sources that appear on the Web.

REFERENCES

- Curtis, A., H. Nicolson, D. Halliday, J. Trampert, and B. Baptie, 2009, Virtual seismometers in the subsurface of the Earth from seismic interferometry: *Nature Geoscience*, **2**, no. 10, 700–704, [doi:10.1038/ngeo615](https://doi.org/10.1038/ngeo615).
- Golub, G., and C. van Loan, 1996, *Matrix computations*: Johns Hopkins University Press.
- Hansen, P. C., M. E. Kilmer, and R. Kjeldsen, 2006, Exploiting residual information in the parameter choice for discrete ill-posed problems: *BIT*, **46**, no. 1, 41–59, [doi:10.1007/s10543-006-0042-7](https://doi.org/10.1007/s10543-006-0042-7).
- Melo, G., and A. Malcolm, 2011, Microquake seismic interferometry with SVD enhanced Green's function recovery: *The Leading Edge*, **30**, 556–562.
- Melo, G., A. Malcolm, D. Mikessel, and K. van Wijk, 2010, Using SVD for improved interferometric Green's functions: 80th Annual International Meeting, SEG, Expanded Abstracts, **29**, 3986–3990.
- Philippe, F. D., C. Prada, J. de Rosny, D. Clorennec, J.-G. Minonzio, and M. Fink, 2008, Characterization of an elastic target in a shallow water waveguide by decomposition of the time-reversal operator: *Journal of the Acoustical Society of America*, **124**, no. 2, 779–787, [doi:10.1121/1.2939131](https://doi.org/10.1121/1.2939131).
- Sacchi, M. D., T. J. Ulrych, and Magnuson, 1998, Eigen-image analysis of common offset sections: Signal-to-noise enhancement and prestack data compression.
- Snieder, R., 2004, Extracting the green's function from correlation of coda waves: A derivation based on stationary phase: *Physical Review E: Statistical, Nonlinear, and Soft Matter Physics*, **69**, no. 4, 046610, [doi:10.1103/PhysRevE.69.046610](https://doi.org/10.1103/PhysRevE.69.046610).
- Ulrych, T. J., S. Freire, and P. Siston, 1988, Eigenimage processing of seismic sections: 58th Annual International Meeting, SEG, Expanded Abstracts, **7**, 1261–1265.
- Waldhauser, F., and W. L. Ellsworth, 2000, A double-difference earthquake location algorithm: Method and application to the northern Hayward fault, California: *Bulletin of the Seismological Society of America*, **90**, no. 6, 1353–1368, [doi:10.1785/0120000006](https://doi.org/10.1785/0120000006).
- Zhang, H., and C. H. Thurber, 2003, Double-difference tomography: The method and its application to the Hayward fault, California: *Bulletin of the Seismological Society of America*, **93**, no. 5, 1875–1889, [doi:10.1785/0120020190](https://doi.org/10.1785/0120020190).